Biochimica et Biophysica Acta 1834 (2013) 2520–2527

Contents lists available at ScienceDirect

Biochimica et Biophysica Acta

journal homepage: www.elsevier.com/locate/bbapap

Schistosoma mansoni NAD$^+$ catabolizing enzyme: Identification of key residues in catalysis

Isabelle Kuhn [a], Esther Kellenberger [b], Francis Schuber [a], Hélène Muller-Steffner [a,*]

[a] Laboratoire de Conception et Application de Molécules Bioactives, UMR 7199 CNRS–Université de Strasbourg, Faculté de Pharmacie, Medalis Drug Discovery Center, 74 route du Rhin, 67400 Illkirch, France

[b] Laboratoire d'Innovation Thérapeutique, UMR 7200 CNRS–Université de Strasbourg, Faculté de Pharmacie, Medalis Drug Discovery Center, 74 route du Rhin, 67400 Illkirch, France

ARTICLE INFO

Article history:
Received 4 June 2013
Received in revised form 21 August 2013
Accepted 5 September 2013
Available online 12 September 2013

Keywords:
Schistosoma mansoni
*Sm*NACE
CD38
Docking

ABSTRACT

Schistosoma mansoni NAD$^+$ catabolizing enzyme (*Sm*NACE), a distant homolog of mammalian CD38, shows significant structural and functional analogy to the members of the CD38/ADP-ribosyl cyclase family. The hallmark of *Sm*NACE is the lack of ADP-ribosyl cyclase activity that might be ascribed to subtle changes in its active site. To better characterize the residues of the active site we determined the kinetic parameters of nine mutants encompassing three acidic residues: (i) the putative catalytic residue Glu202 and (ii) two acidic residues within the 'signature' region (the conserved Glu124 and the downstream Asp133), (iii) Ser169, a strictly conserved polar residue and (iv) two aromatic residues (His103 and Trp165). We established the very important role of Glu202 and of the hydrophobic domains overwhelmingly in the efficiency of the nicotinamide–ribosyl bond cleavage step. We also demonstrated that in sharp contrast with mammalian CD38, the 'signature' Glu124 is as critical as Glu202 for catalysis by the parasite enzyme. The different environments of the two Glu residues in the crystal structure of CD38 and in the homology model of *Sm*NACE could explain such functional discrepancies. Mutagenesis data and 3D structures also indicated the importance of aromatic residues, especially His103, in the stabilization of the reaction intermediate as well as in the selection of its conformation suitable for cyclization to cyclic ADP-ribose. Finally, we showed that inhibition of *Sm*NACE by the natural product cyanidin requires the integrity of Glu202 and Glu124, but not of His103 and Trp165, hence suggesting different recognition modes for substrate and inhibitor.

1. Introduction

We have recently identified a Schistosoma mansoni NAD+ catabolizing enzyme (SmNACE) expressed as a GPI-anchored glycoprotein on the outer tegument of the adult form of this parasitic platyhelminth that represents a potentially attractive drug target to fight schistosomiasis [1]. *Sm*NACE belongs to the family of CD38/ADP-ribosyl cyclases which are key enzymes in the production of Ca^{2+}-mobilizing messengers such as cyclic ADP-ribose (cADPR) and NAADP$^+$ [2,3]. The catalytic transformation of NAD$^+$ by these enzymes involves a unique ADP-ribosyl reaction intermediate that can evolve into different products. As shown in Fig. 1, the hydrolysis reaction converts NAD$^+$ into ADPR, whereas the cyclization reaction forms cADPR [4,5]. The partition between the two reaction pathways varies within this enzyme family: the mollusc *Aplysia californica* ADP-ribosyl cyclase overwhelmingly catalyses cyclization whereas mammalian CD38 predominantly catalyze hydrolysis. *Sm*NACE is however virtually unable to catalyze the formation of cADPR from NAD$^+$, i.e. it is almost exclusively a NAD$^+$glycohydrolase [1] (Fig. 1). The efficient NAD$^+$ hydrolysis activity present at the surface of the adult parasite presumably scavenges the host's circulating free NAD$^+$, thereby impacting on the NAD$^+$-dependent pathways of the human immune system [6,7].

*Sm*NACE, and more generally the members of the CD38/ADP-ribosyl cyclase family, are small proteins of approximately 300 amino acids, with distinctive sequence signatures and a typical 3D structure maintained by five disulfide bridges (Fig. 2). The molecular architecture observed in the crystal structure of human [8], bovine [9] and murine CD38 [10], human CD157 [11] and *A. californica* cyclase [12] consists of two lobes that define a cleft. At the bottom of this cleft lies the active site which is formed by well conserved amino acids that define a binding pocket with a typical shape and distinctive properties (Fig. 3). In the absence of *Sm*NACE crystals the aim of this work was to validate the putative active site of this enzyme obtained by homology modeling [13]. If the active site of *Sm*NACE overall matches the characteristics of the members of the CD38/ADP-ribosyl cyclase family, specific traits in its sequence have however raised the hypothesis that fine tuning of the partition reaction mechanism is correlated to subtle changes in the nature of amino acids in the active site. Accordingly we have previously

Abbreviations: *Sm*NACE, *Schistosoma mansoni* NAD$^+$ catabolizing enzyme; ADPR, ADP-ribose; cADPR, cyclic ADP-ribose; NAD$^+$, nicotinamide adenine dinucleotide; NAADP$^+$, nicotinic acid adenine dinucleotide; GPI, glycosyl phosphatidylinositol

* Corresponding author. Tel.: +33 368 85 41 69; fax: +33 368 85 43 06.
E-mail address: steffner@unistra.fr (H. Muller-Steffner).

1570-9639/$ – see front matter © 2013 Elsevier B.V. All rights reserved.
http://dx.doi.org/10.1016/j.bbapap.2013.09.002

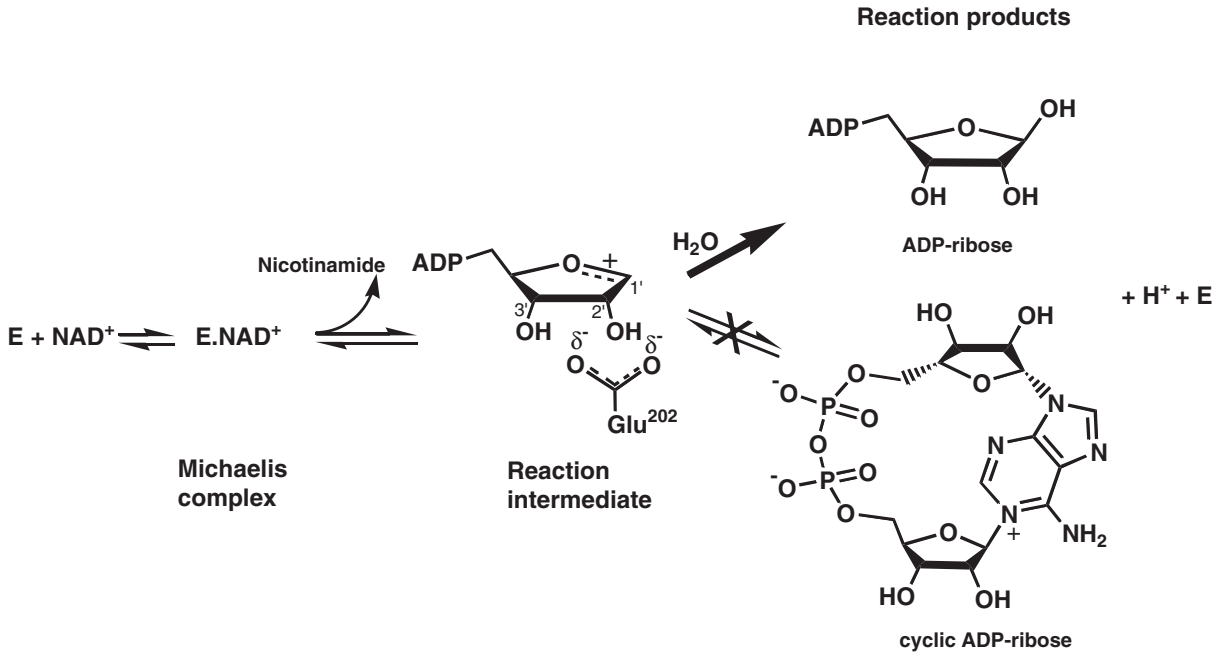

Fig. 1. Reaction mechanism of the transformation of NAD^+ by CD38/ADP-ribosyl cyclases. The cleavage of the nicotinamide–ribosyl bond of NAD^+ leads to the formation of an ADP-ribosyl intermediate that partitions between different acceptors to give the reaction products [4,5]. In contrast to CD38, the ADP-ribosyl cyclization step is hardly detectable in *Sm*NACE (indicated by a cross). For the sake of simplicity, an ion-pair stabilized ADP–ribooxocarbenium ion was drawn as transient intermediate; however the occurrence of a covalent acylal intermediate with the catalytic Glu202 cannot be excluded.

investigated the effect of the replacement in *Sm*NACE of His103, which is a Trp in all other known members of the CD38/ADP-ribosyl cyclase family (e.g. Trp125 in human CD38) [13]. The kinetic parameters of the H103W mutant revealed that the downsizing of this aromatic side chain is responsible for the incapacity of the native enzyme to catalyze the cyclization reaction. In the present work we have probed the functional role of the other putative key residues in the active site of *Sm*NACE. In particular, we designed and determined the kinetic parameters of nine single point mutants corresponding to the following positions: (i) the putative catalytic residue Glu202, (ii) two acidic residues found within and downstream the so-called 'signature' region (Glu124 and Asp133), (iii) a strictly conserved Ser residue (Ser169) found in the active site of CD38 and ADP-ribosyl cyclases, and (iv) two aromatic residues, His103 and the strictly conserved tryptophan at position 165. Finally, since the deciphering of the structural features of the *Sm*NACE active site could provide insights for the design of prospective therapeutic agents, the mutants were also tested in presence of cyanidin, a low micromolar competitive inhibitor of wild type *Sm*NACE [14].

2. Material and methods

2.1. Construction of the expression vector

The primary nucleotide sequence of *Sm*NACE was optimized for yeast codon usage and resynthesized (GenScript, Piscataway, USA). To produce recombinant soluble *Sm*NACE in yeast, the 5′-leader sequence and the GPI-anchor sequences were eliminated. The remaining core ectodomain sequence was cloned into the *Pichia pastoris* expression vector pPICZαA into the EcoRI and XbaI sites leading to the expression of soluble *Sm*NACE (residues 20–275) as previously described [1]. A *myc*-epitope fused to a His_6-tag is coded by the vector at the C-terminus of this construct to facilitate purification of the recombinant protein.

2.2. Site-directed mutagenesis of SmNACE

The different *Sm*NACE mutant constructs were generated by PCR (kit 'quick-change site-directed mutagenesis', Stratagene) with *Pfu*-DNA polymerase using the primers listed below (mutated bases in bold): H103A 5′AGCAGTACTTC**GCT**AGCCAGGTGATG3′; H103F 5′AGCAGTA CTTC**TTC**AGCCAGGTGATC3′; E202A 5′GGAAAAATT**GCT**TTGCCATTGTT G3′; E124A 5′GTAGATCTTTG**GCT**ACAACAATTTCC3′; W165A 5′GTGCAC GCCTTC**GCT**CAGTCCGCCTCC3; W165F 5′GTGCACGCCTTC**TTC**CAGTCC GCCTCC3′; D133A 5′GTTACTTGTTT**GCT**GAATTGAATTG3′; S169A 5′ TGGCAGTCCGCC**GCT***GCC*GAGTACGCC3′. To avoid translational misincorporation during protein synthesis, mutations were systematically obtained by at least a double-base pair substitution. All constructs were verified by DNA sequencing of the clones using the 5′ and 3′ AOX primers (Invitrogen).

2.3. Expression and purification of the recombinant proteins

The different *Sm*NACE mutants were expressed in *P. pastoris*. The expressed His-tagged mutants secreted in the medium by the yeast were purified in a single step alternatively on HiTrap Blue HP (GE Healthcare) or Ni^{2+}-affinity gel (Hi-Trap Chelating HP GE Healthcare) columns (1 mL) as previously described [13]. To prevent any cross-contamination, each mutant was purified on a dedicated affinity column. Protein concentrations were determined by the OD at 280 nm and by the BCA protein assay (Pierce) using BSA as standard.

2.4. Enzyme assays and kinetic studies

The enzyme activity was measured at 20 μM NAD^+ as described previously [1] by following the product formation by HPLC on a 300 × 3.9 mm μBondapack C_{18} column (Waters). The isocratic elution was performed at a flow rate of 1 mL/min (10 mM ammonium phosphate buffer, pH 5.5, with 1.2% (v/v) acetonitrile). In some cases [adenosine-U-^{14}C] NAD^+ (2×10^5 dpm) was added to the unlabeled substrate. The eluted compounds were detected by absorbance recordings at 260 nm and by radiodetection (Flo-one, Packard Radiometric Instruments) when using [^{14}C] NAD^+ [1,13].

Kinetic parameters K_m and V_m were determined from the plots of the initial rates of ADP-ribose formation as a function of substrate concentration (7 to 8 points) according to Michaelis–Menten kinetics, using a